



# Programmable biofilm-based materials from engineered curli nanofibres

## Citation

Nguyen, Peter Q., Zsafia Botyanszki, Pei Kun R. Tay, and Neel S. Joshi. 2014. "Programmable Biofilm-Based Materials from Engineered Curli Nanofibres." *Nature Communications* 5 (September 17): 4945. doi:10.1038/ncomms5945.

## Published Version

doi:10.1038/ncomms5945

## Permanent link

<http://nrs.harvard.edu/urn-3:HUL.InstRepos:14350457>

## Terms of Use

This article was downloaded from Harvard University's DASH repository, and is made available under the terms and conditions applicable to Other Posted Material, as set forth at <http://nrs.harvard.edu/urn-3:HUL.InstRepos:dash.current.terms-of-use#LAA>

## Share Your Story

The Harvard community has made this article openly available.  
Please share how this access benefits you. [Submit a story](#).

[Accessibility](#)

1  
2  
3  
4  
5  
6  
7  
8 **Programmable Biofilm-Based Materials from Engineered Curli Nanofibers**

9  
10  
11 Peter Q. Nguyen<sup>1,2</sup>, Zsafia Botyanszki<sup>2,3</sup>, Pei Kun R. Tay<sup>1,2</sup> and Neel S. Joshi<sup>1,2\*</sup>

12  
13 School of Engineering and Applied Sciences<sup>1</sup>,  
14 Wyss Institute for Biologically Inspired Engineering<sup>2</sup>,  
15 Department of Chemistry and Chemical Biology<sup>3</sup>,  
16 Harvard University, Cambridge, MA 02138, USA.  
17  
18  
19  
20  
21  
22  
23  
24  
25  
26  
27  
28  
29  
30  
31  
32

33 \*Corresponding Author: Dr. Neel S. Joshi  
34 School of Engineering and Applied Sciences /  
35 Wyss Institute for Biologically Inspired Engineering  
36 Harvard University  
37 Cambridge, MA 02138, USA.  
38  
39 Tel: (617) 432-7732  
40 E-Mail: njoshi@seas.harvard.edu  
41  
42  
43

## Abstract

The significant role of biofilms in pathogenicity has spurred research into preventing their formation and promoting their disruption, resulting in overlooked opportunities to develop biofilms as a synthetic biological platform for self-assembling functional materials. Herein we present “Biofilm-Integrated Nanofiber Display” (BIND) as a strategy for the molecular programming of the bacterial extracellular matrix material by genetically appending peptide domains to the amyloid protein CsgA, the dominant proteinaceous component in *E. coli* biofilms. These engineered CsgA fusion proteins are successfully secreted and extracellularly self-assemble into networks of amyloid nanofibers that retain the functions of the displayed peptide domains. We show the use of BIND to confer diverse artificial functions to the biofilm matrix, such as nanoparticle biotemplating, substrate adhesion, covalent immobilization of proteins, or a combination thereof. BIND is a versatile nanobiotechnological platform for developing robust interfacial materials with programmable functions, demonstrating the potential of utilizing biofilms as large-scale designable biomaterials.

## 1 Introduction

2 Advances in our understanding of bacterial systems in the past century have expanded the  
3 role of the microbe from being regarded solely as a health threat to being exploited as a  
4 genetically programmable factory for the production of biomolecules and chemicals. We view  
5 bacterial biofilms as embarking on a similar trajectory vis-à-vis functional advanced materials.  
6 The majority of bacteria in the natural world exist as biofilms: organized communities of cells  
7 ensconced in a network of extracellular matrix (ECM) composed of polysaccharides, proteins,  
8 nucleic acids, and other biomolecular components<sup>1</sup>. This self-generated ECM protects bacteria  
9 from environmental rigors and mediates substrate adhesion, thus promoting microbial  
10 persistence and pathogenicity. Hence, the majority of biofilm research has focused on their  
11 eradication due to the negative roles biofilms play in clinical infection<sup>2</sup>.

12 We envision instead the domestication of biofilms as a platform for programmable and  
13 modular self-assembling extracellular nanomaterials, with the bacterium serving as a living  
14 foundry for the synthesis of raw building blocks, their assembly into higher order structures upon  
15 secretion, and the maintenance of the material as a whole over time. While there has been some  
16 investigation into the use of biofilms for beneficial purposes such as energy generation<sup>3</sup>,  
17 wastewater treatment<sup>4</sup> and biotransformations<sup>5,6</sup>, these studies have primarily focused on altering  
18 the population of the biofilm microbial consortia rather than the ECM material itself. Another  
19 example is recent exciting work from the Wood group, in which they describe the design of  
20 synthetic genetic circuits that modulate the population balance in a dual-species biofilm to  
21 control biofilm formation and dispersal based on quorum-sensing<sup>7</sup>.

22 Our approach to engineering the biofilm ECM material for practical applications focuses  
23 on the curli system – the primary proteinaceous structural component of *E. coli* biofilms. Curli



are highly robust functional amyloid nanofibers with a diameter of ~4-7 nm that exist as extended tangled networks encapsulating the cells. Curli are formed from the extracellular self-assembly of CsgA, a small secreted 13-kDa protein. A homologous outer-membrane protein, CsgB, nucleates CsgA assembly and also anchors the nanofibers to the bacterial surface. Detached curli fibers can also exist as non-cell associated structural components of the ECM. The curli genes exist as two divergently transcribed operons (*csgBAC* and *csgDEFG*)<sup>8</sup>, whose seven products mediate the structure (CsgA), nucleation (CsgB), processing (CsgE, F), secretion (CsgC, G), and direct transcriptional regulation (CsgD) of curli nanofibers.

The curli system exhibits numerous features that make it an ideal platform for the type of materials engineering by way of synthetic biology that we envision. First, since the curli nanofiber is composed primarily from the self-assembly of one small protein, it presents a tractable entry point towards creating a large diversity of biofilm extracellular matrices with conventional genetic engineering methods. In contrast, it would be more difficult to engineer the exopolysaccharide component of biofilms, as polysaccharide synthesis is often tied to multi-step pathways with a limited tolerance for chemically diverse monomers compared to the protein synthetic machinery. Second, the functional amyloid fibers formed by CsgA are extremely robust, being able to withstand boiling in detergents<sup>9</sup> and extended incubation in solvents, increasing their potential utility in harsh environments. Similar amyloid nanofibers have been shown to have a strength comparable to steel and a mechanical stiffness comparable to silk<sup>10</sup>, suggesting that biofilms with high amyloid content would be able to withstand mechanically demanding environments. Third, functional amyloid fibrils are abundant in many naturally occurring bacterial biofilms and can constitute up to 10-40% of the total biovolume of a biofilm<sup>11</sup>, indicating that curli can be artificially engineered to comprise a significant portion of

1 the biofilm. In addition, although analogous extracellular functional amyloids are produced by  
2 many bacteria, the curli system is currently the best studied and is native to the canonical model  
3 bacterium *E. coli*, making it an attractive starting platform for the development of engineered  
4 materials. Finally, recent findings have shown that the curli system can be used to efficiently  
5 export natively unfolded polypeptides and was capable of expressing a functional camelid  
6 antibody fragment, suggesting that the curli system can be used in a broad and modular way for  
7 the display of various functional peptides throughout the *E. coli* biofilm ECM, as we present  
8 here<sup>12,13</sup>.

9         The BIND system enables the precise genetic programming of the *E. coli* biofilm  
10 extracellular matrix material by fusing functional peptide domains to the CsgA protein (Fig. 1).  
11 We demonstrate that the chimeric CsgA variants are secreted by the native cellular export  
12 machinery and assemble into networks of curli fibers that resemble the wild-type system. We  
13 also show that this technique is compatible with a wide range of peptide domains of various  
14 lengths and secondary structures. Lastly, we demonstrate that the peptide domains maintain their  
15 function after secretion and assembly and confer artificial functions to the biofilm as a whole.  
16 Very recently, Chen et al. have demonstrated a parallel curli-based system similar to our BIND  
17 concept, and show controlled multiscale patterning of single amyloid fibers and the use of  
18 engineered curli for the organization of gold nanoparticles and quantum dots for nanoelectronics  
19 applications<sup>14</sup>. Herein, we expand on the functions that can be engineered into curli nanofibers  
20 by demonstrating three broad functions that we artificially introduce into the *E. coli* biofilm  
21 ECM: inorganic nanoparticle templating, specific abiotic substrate adhesion, and the site-specific  
22 covalent immobilization of an arbitrary functionalized recombinant protein.

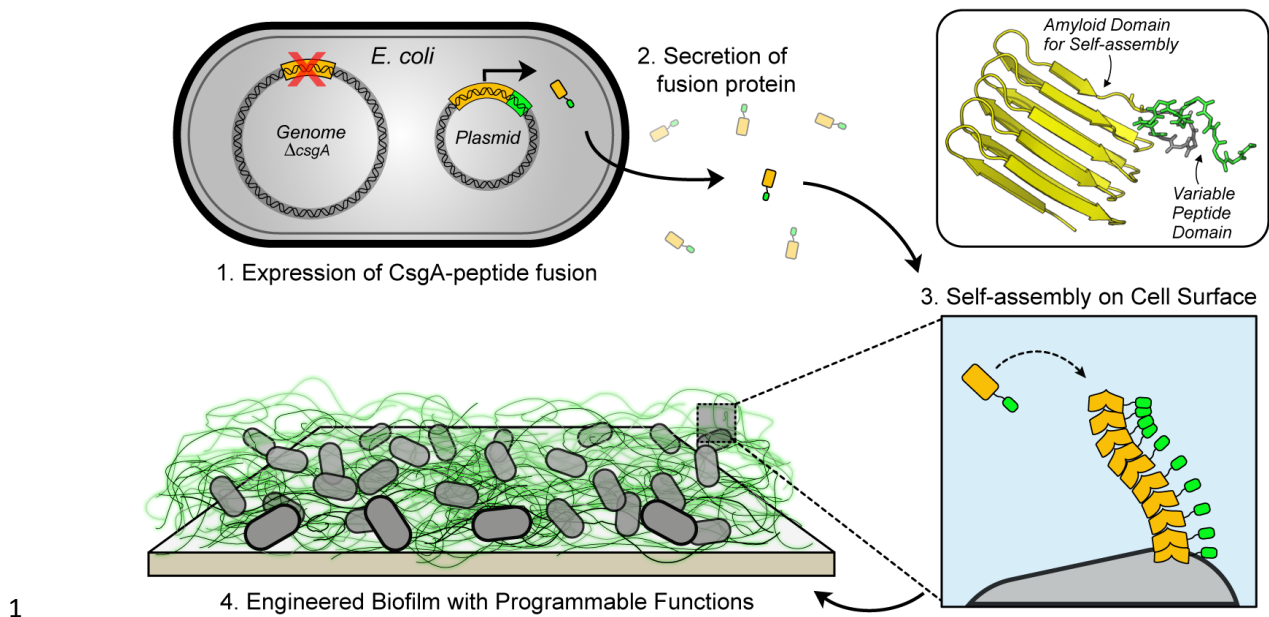


**Figure 1 | Genetic programming and modularity of the BIND system.** In the BIND platform,  $\Delta$ csgA cells heterologously express and secrete fusion proteins consisting of an amyloidogenic domain (CsgA, shown in orange) and a functional peptide domain (green). This secreted fusion protein self-assembles into an extracellular network of amyloid nanofibers that are anchored onto the cell surface, resulting in a biofilm material with programmed non-natural functions. A three-dimensional protein model is shown of the self-assembling and functional peptide domains, using homology model protein threading of the CsgA sequence onto an AgfA structure. An example peptide domain, SpyTag (see Table 1), is shown in green and the 6-residue flexible linker in gray. The peptide structure was predicted using PepFold and all structural manipulation performed in PyMol.

## Results

**Determination of an optimal peptide fusion site for CsgA.** In order to determine suitable fusion points to append peptides to CsgA, we generated a library (Fig. 2a) consisting of N- and C-terminal fusions to a test peptide domain designated MBD (for Metal Binding Domain). The MBD peptide has been shown to bind strongly to stainless steel surfaces and is derived from a segment of the *Pseudomonas aeruginosa* type IV pilus<sup>15</sup>. CsgA-terminal fusions were chosen to allow for the integration of both linear and circularly constrained peptides. Three variants were prepared for each terminus with varying glycine-serine flexible linker lengths. We used the standard amyloid-staining colorimetric dye, Congo Red<sup>16</sup> (CR), to determine the extent of curli

1 production for the various mutants. The *csgA* variants were expressed in the model *E. coli csgA*  
2 deletion strain LSR10 (MC4100:: $\Delta csgA$ ) that retains the remaining curli processing machinery  
3 under native regulation<sup>8</sup>. This strain has previously been used in numerous studies on the curli  
4 system as it has been shown to not produce flagella, cellulose, or LPS O-polysaccharides,  
5 making it ideal for curli complementation studies<sup>17-19</sup>. Thus, LSR10 was chosen as a model strain  
6 for developing BIND in part because any colorimetric signal obtained from CR staining could be  
7 attributed to the presence of heterologously produced curli fibers, as opposed to cellulose or  
8 other biofilm components that may have the capability to bind CR non-specifically<sup>20</sup>. Likewise,  
9 any extracellular fibers observed by transmission electron microscopy (TEM) and scanning  
10 electron microscopy (SEM) ultrastructural characterization can be attributed solely to the self-  
11 assembly of heterologously engineered CsgA fusion mutants.

12         The CR staining assay of the MBD insertion library indicated only the C3 fusion site with  
13 the longest C-terminal linker between CsgA and MBD was able to form an appreciable amount  
14 of amyloid fibers (Fig. 2b), albeit at a lower amount than the wild-type CsgA. It is possible that  
15 the N-terminal fusions had impaired secretion as a result of their proximity to the CsgG-specific  
16 export recognition sequence. Ultrastructural characterization by SEM (Fig. 2n) and TEM  
17 (Supplementary Fig. S3k and Supplementary Fig. S4j) of the C3 mutant curli nanofibers  
18 confirmed that they exhibited morphology similar to that of the wild-type CsgA fibers.

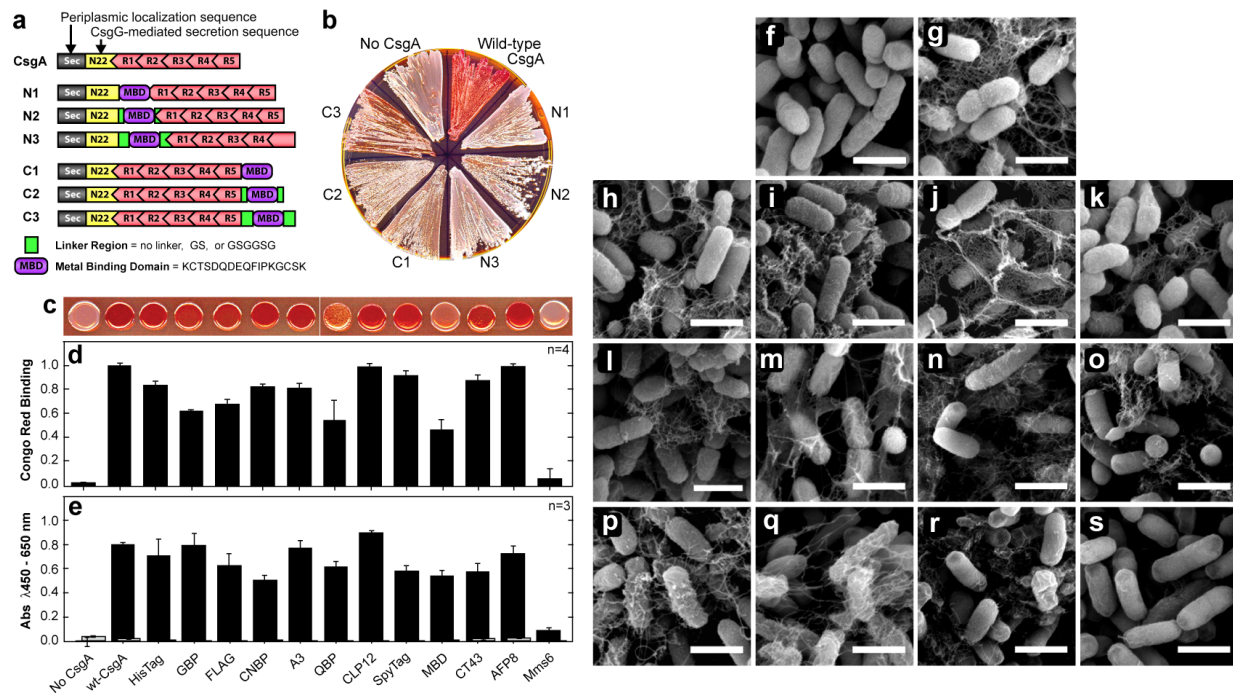


**Figure 2 | Genetic engineering of the BIND platform.** (a) A library of CsgA fusion mutants in which the MBD peptide insert (purple) was placed at the N- or C-terminus of the curlin repeat domains (red) and flanked by a 6-residue linker, 2-residue linker, or no linker (green). (b) The MBD insert library was transformed into LSR10 (MC4100,  $\Delta csgA$ ) cells and streaked onto YESCA-Congo Red induction plates. Red staining indicates amyloid production. (c) A representative set of culture spots of a BIND library consisting of 12 various functional peptides on YESCA-Congo Red induction plates (enumerated in Table 1). (d) Quantitative Congo Red values were obtained from quadruplicate YESCA-CR spotted cultures using intensity quantitation (ImageJ) measurements of the relative amyloid produced for each CsgA-peptide fusion, normalized to wild-type CsgA. (e) Whole-cell filtration ELISA using an anti-CsgA antibody (black bars); secondary antibody-only controls are shown as grey bars. Each experiment was performed in triplicate. FE-SEM images of the peptide fusion BIND library transformed into LSR10 (MC4100,  $\Delta csgA$ ) cells with no CsgA (f), wt-CsgA (g), and the BIND peptide panel (see Table 1): HIS (h), GBP (i), FLAG (j), CNBP (k), A3 (l), CLP12 (m), QBP1 (n), SpyTag (o), MBD (p), CT43 (q), AFP8 (r), and Mms6 (s). All scale bars are 1  $\mu$ m.

**Various CsgA-peptide fusions retain amyloid self-assembly function.** Having identified the C3 fusion site as suitable for the expression of peptides on the CsgA scaffold, we next created a library of 12 various peptide domain fusions to test the effect of peptide length and structure on secretion and assembly. The library members, detailed in Table 1, range in length from 7 to 59 amino acids and encode a wide variety of functions such as binding to various inorganic substrates (GBP, CNBP, QBP, MBD, and AFP8), nucleation of mineral and metallic

nanostructures (A3, CLP12, CT43, and Mms6), and a highly specific catalytic interaction with a protein (SpyTag)<sup>15,21-31</sup>. Each peptide domain was cloned as C-terminal fusions to CsgA with an intervening six-amino acid flexible linker (Table 1) and these plasmids were expressed in LSR10 cells to produce 12 different BIND biofilms.

Table 1   Functional Peptide Library Incorporated into BIND					
Peptide	Sequence	Length (aa)	Type	Specific Function	Reference
HIS	HHHHHH	6	Affinity Tag	Affinity Tag	21
GBP	EPLQLKM	7	Substrate Binding	Graphene edge binding	22
FLAG	DYKDDDDK	8	Affinity Tag	Affinity Tag	23
CNBP	HSSYWYAFNNKT	12	Substrate Binding	Carbon nanotube binding	24
A3	AYSSGAPMPPF	12	Substrate Binding	Gold surface binding	25
CLP12	NPYHPTIPQSVH	12	Mineral templating	Hydroxyapatite nucleation	26
QBP1	PPPWLPYMPWWS	12	Substrate Binding	Quartz/Glass binding	27
SpyTag	AHIVMVDAYKPTK	13	Protein Display	Covalent capture/display of proteins	28
CT43	CGPAGDSSGVDSRVGPC	18	NP templating	ZnS templating	29
MBD	KCTSDQDEQFIPKGCSSGSGSG	23	Substrate Binding	Binding to stainless steel surfaces	15
AFF8	DTASDAAAAAALTAANAKAAELTAANAAAAAATAR	37	Substrate Binding	Ice crystal binding	30
Mms6	GGTIWTGKGLGLGLGLGAWGPILGVVGAGAVYAYMKSRDIESAQSDDEEVELRDALA	59	NP templating	Magnetite templating	31

Relative differences in curli production between library members were monitored by measuring the staining intensity of transformants spotted on CR plates (Fig. 2c,d). Overall, most small peptide fusions were tolerated by the curli export machinery and could successfully assemble into extracellular amyloid networks as evidenced by greater CR staining of all peptide fusions compared to the empty plasmid control. The only mutant for which there was no positive CR staining was the 59-amino acid Mms6 protein domain, confirming previous findings that polypeptides with long sequences or inherent structure may not be exported efficiently through the CsgG outer membrane transporter, which has a pore size of 2 nm<sup>13,32</sup>. A more specific assessment of the amyloid-nature of proteins is provided from birefringence of the CR-stained material observed under polarized light<sup>33-35</sup>. Cell masses of the BIND colonies from YESCA-CR plates were analyzed by polarization microscopy (Supplementary Fig. S1). Most of the BIND variants exhibited birefringence characteristic of amyloids, although the intensity of the birefringence varied. The no curli control and Mms6-BIND samples showed no birefringence, as expected. Surprisingly, the CLP12- and QBP-BIND samples showed very low levels of

1 birefringence, although they have high levels of CR binding. We posit that this is due to the  
2 amyloid fibers being highly dispersed or the presence of these peptides altering the binding mode  
3 of the CR such that birefringence is suppressed. To validate that the CR staining is due to the  
4 presence of extracellular curli nanofibers, we performed whole-cell filtration ELISAs using anti-  
5 CsgA antibodies (Figure 2e). Only extracellular curli fibers retained by the 0.22  $\mu\text{m}$  filter would  
6 generate a CsgA-positive signal. The whole-cell ELISA data correlates with the CR staining  
7 results, confirming that the CsgA fusions, with the exception of the Mms6 fusion, are secreted  
8 extracellularly and are present as high molecular-weight assemblies. To rule out the possibility  
9 that these extracellular amyloids are due to the secretion and assembly of partially proteolyzed  
10 CsgA fusion proteins and not the desired full-length CsgA fusion proteins, we isolated the  
11 extracellular fractions of induced BIND colonies and subjected this fraction to SDS  
12 solubilization. The SDS-insoluble fraction was collected by ultracentrifugation and dissolved in  
13 hexafluoroisopropanol (HFIP) to disassemble the curli fibers into their monomeric components.  
14 MALDI-TOF/TOF analysis of the resulting dissolved samples confirms the presence of mass  
15 peaks that correlate with the predicted mature CsgA fusion proteins in all of the samples except  
16 for the no curli control and the Mms6-BIND sample (Supplementary Fig. S2). Although this  
17 does not rule out potential proteolysis events, it does demonstrate that the extracellular fraction  
18 contains the CsgA fusion proteins that are in an SDS-insoluble state, suggesting that the desired  
19 proteins are assembled into amyloid structures. To further confirm the presence of curli  
20 nanofibers and rule out unstructured extracellular aggregates in the BIND biofilms, we  
21 extensively analyzed the ultrastructure of the curli biofilms using SEM (Fig. 2f-s) and TEM  
22 (Supplementary Fig. S3). For the CR-positive transformants, fine nanofibers associated with the  
23 cells were observed which are similar in morphology to wild-type CsgA. High magnification

TEM analysis of the BIND nanofibers revealed that they have a diameter of 4-7 nm, consistent with that previously reported for curli nanofibers<sup>36</sup> (Supplementary Fig. S4). The BIND nanofibers displayed a characteristic tangled morphology and were observed to be closely associated with the cell surface or sometimes existing as free-floating masses. No extracellular fibers were observed for either the empty plasmid control or the Mms6-BIND biofilm (Fig. 2f,s and Supplementary Fig. S3a,n), corroborating the lack of CR staining and whole-cell ELISA signals for these samples. We additionally performed immunogold labeling of the BIND biofilms expressing the CsgA-FLAG fusion protein, using an anti-FLAG antibody. The immunogold TEM images show localization of the gold nanoparticles to the curli fiber tangles, confirming both the presence and accessibility of the FLAG peptide domain (Supplementary Fig. S5). In sum, the CR staining and CR birefringence experiments demonstrate the presence of extracellular amyloid, the whole-cell filtration ELISA data indicate that the CsgA fusions are present as extracellular assemblies, the MALDI analysis confirms the presence of SDS-insoluble extracellular material correlating in mass to the expected fusion proteins, and electron microscopy imaging of the BIND biofilms provides ultrastructural verification of the nanofibrillar morphology of the BIND ECM. Thus, peptides of arbitrary sequence and function could be efficiently displayed as C-terminal fusions to CsgA for extracellular self-assembly into functionalized curli nanofibers.

The true value of the BIND system is in its ability to perform as an expansive interfacial biomaterial whose function can be genetically programmed in a modular fashion. As a demonstration of some of these capabilities, we selected three peptides from Table 1 (FLAG, A3, MBD, and SpyTag) with diverse functions and tested their ability to introduce these new functions into curli-producing biofilms. Specifically, we investigated the ability to program



1 biotemplating of inorganic nanoparticles (A3), enhanced adhesion to abiotic surfaces (MBD),  
2 and covalent immobilization of full-length proteins into the BIND biofilms (SpyTag). We also  
3 examined the generation of multifunctional BIND biofilms (FLAG and SpyTag). For these  
4 functional studies we chose a different cell strain as a chassis for robust curli production, a  
5 previously developed *csgA* deletion mutant of the *E.coli* K-12 strain PHL628<sup>37</sup>. Although they  
6 also produce cellulose, which made them unsuitable for the initial characterization of the BIND  
7 platform, the PHL628 (MG1655 *malA-Kan ompR234* ) cells are superior to the LSR10 strain for  
8 curli production due to a single point mutation in the OmpR protein which enhances expression  
9 of the entire curli operon by ~3.5x, resulting in substantial amounts of curli production<sup>38</sup>. This  
10 phenotype is ideal for generating expansive amyloid-rich ECM for functional analysis; plasmid-  
11 based overexpression of heterologous BIND variants in a  $\Delta csgA$  PHL628 knockout mutant  
12 (hereafter referred to just as PHL628) is likely to prevent accumulation of the fusion proteins  
13 intracellularly by providing a high basal expression of the proteins required for efficient  
14 processing and secretion of the CsgA fusions. Expression of the entire BIND peptide library in  
15 PHL628 cells resulted in similar relative curli production patterns as determined by CR binding  
16 in comparison to the LSR10 strain (Supplementary Fig. S6). We also performed whole-cell  
17 filtration ELISAs on the FLAG-, A3-, SpyTag-, and MBD-BIND biofilms to show that the CsgA  
18 protein is exported and assembles into a high molecular-weight extracellular material  
19 (Supplementary Fig. S7a,c,e,g). Furthermore, MALDI-TOF/TOF analysis of the SDS-insoluble  
20 purified extracellular material shows mass peaks that correspond that that of the expected fusion  
21 proteins, suggesting that they are present and unproteolyzed as amyloid fibrils in the ECM  
22 (Supplementary Fig. S7b,d,f,h).

**Silver nanoparticle templating onto A3-BIND nanofibers.** Engineered peptides functionalized onto the ECM can also be used to promote materials templating, which we demonstrate using BIND composed of a CsgA-A3 fusion expressed in PHL628 cells. The A3 peptide was previously developed by phage display to bind silver and has been shown to control the templating of silver nanoparticles<sup>25</sup>. The wild-type CsgA biofilm did not appreciably template silver nanoparticles (Fig. 3a). In contrast, the A3-BIND biofilms show an enhanced ability to bind to growing silver nanoparticles from a solution of AgNO<sub>3</sub>, as shown by representative TEM images of incubated A3-BIND showing the assembly of nanoparticles throughout the nanofibers. (Fig. 3b-c). These results are reproducible (Supplementary Fig. S8) and demonstrate the utility of programmable biofilm matrices for the templating and organization of nanoparticles to form one-dimensional nanowires. The resulting nanoparticle-decorated nanofibers show a striking resemblance to naturally occurring metal-reducing extracellular fibers from *Geobacter sulfurreducens*, which have been shown to be electrically conductive<sup>39</sup>, suggesting that BIND-based biotemplating may be a viable strategy for the large-scale *de novo* production of conductive nanowires.

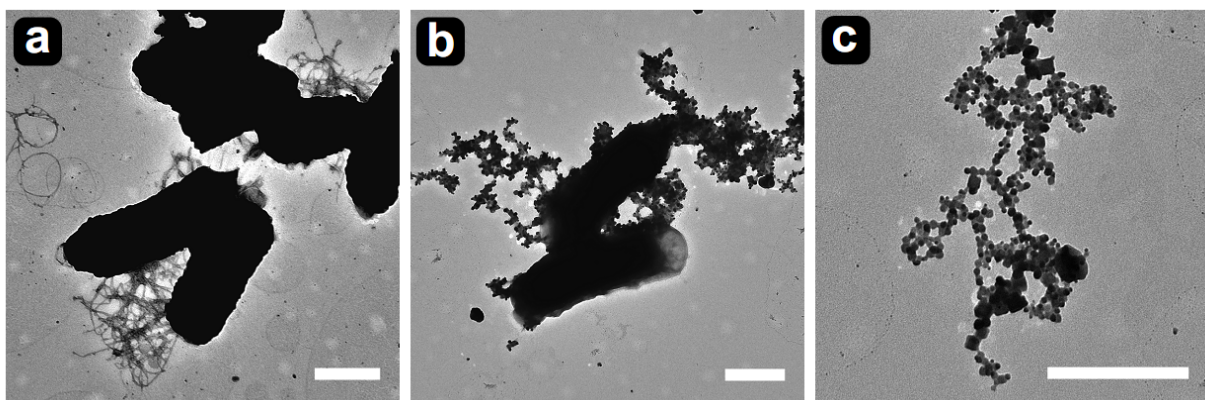


**Figure 3 | Nanoparticle Templating by BIND.** Silver nanoparticles were templated by A3-BIND biofilms incubated in aqueous AgNO<sub>3</sub>. Representative TEM micrographs demonstrate that PHL628  $\Delta csgA$  cells expressing wild-type CsgA (a) shows no nanoparticle templating, whereas A3-BIND (b) templates nanoparticles after incubation in 147mM AgNO<sub>3</sub> for 4 hours. (c) A higher magnification of the Ag nanoparticles organized on A3-BIND nanofilaments is shown. All scale bars are 0.5 microns.

**Programmed BIND substrate adhesion onto 304L stainless steel.** In order to make BIND an efficient platform for developing interfacial materials, it will be critical to tune the nanofiber adhesion to specific abiotic surfaces. As an example of this capability, we tested the adhesion of *E. coli* cells displaying MBD to 304L stainless steel, the most versatile and widely used steel alloy. PHL628 cells expressing the CsgA-MBD mutant were spotted onto 304L MBD mutant were spotted onto 304L coupons (Fig. 4a), allowed to adhere for 48 hours, and then vigorously washed by vortexing at a high setting in aqueous buffer to thoroughly remove non-specifically bound cells. The spotted areas were analyzed by SEM and showed that BIND composed of the CsgA-MBD fusion withstood the washing procedure (Fig. 3b-d), while the no CsgA or wild-type CsgA control cells were washed off the surface (Supplementary Fig. S9). This result demonstrates that BIND programming using MBD is sufficient to impart adhesive function to biofilms that can withstand very rigorous washing conditions. The modularity of the BIND platform lends itself to a plug-and-play approach for the

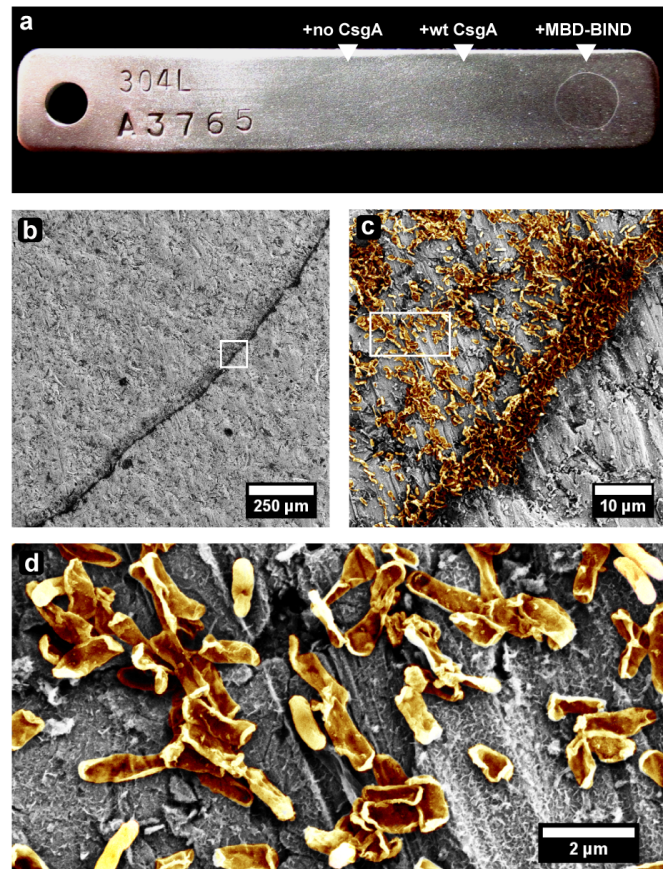


**Figure 4 | BIND biofilms can be programmed to adhere to specific substrates.** (a) Adhesion of PHL628  $\Delta csgA$  cells expressing no CsgA (left), wild-type CsgA (middle), and CsgA-MBD (right) was tested by spotting induced cultures onto a 304L steel coupon and incubating for 48 hours at 4°C. The ring formation is due to cells being drawn to the edges of the droplet during drying, known as the “coffee ring effect”. (b) The MBD-BIND biofilms were analyzed by FE-SEM. (c) magnification of the boxed area in (b) of a false-colored FE-SEM micrograph showing MBD-BIND cells adhered to the 304L surface. (d) magnification of the boxed area in (c) of a false-colored FE-SEM micrograph showing a zoomed-in view of the cell bodies. Due to the vigorous washing process, some of the cell bodies appear damaged.

1 design of programmed biofilm adhesion for applications in bioremediation or chemical synthesis,  
2 where non-specific biofilm growth is viewed as a disadvantage. This capability will be  
3 particularly useful in applications where patterned surfaces are used to spatially control biofilm  
4 formation<sup>40</sup>, or where it is desirable to localize biofilm growth to specific materials and resist  
5 detachment forces, as is often the case in industrial bioreactors<sup>41,42</sup>.

6 **Covalent immobilization of proteins using BIND.** In addition to displaying short peptides, we  
7 reasoned that the utility of the BIND system would be greatly expanded if it could be used to  
8 display full proteins of arbitrary length and dimensions to program the biofilm with artificial  
9 enzymatic, electron transport, or sensing capabilities. We therefore created a two-component  
10 genetically encodable strategy (Fig. 5a) to covalently immobilize proteins onto the BIND  
11 network, using a previously developed split-adhesin system<sup>28</sup> in which a 13-amino acid peptide  
12 (SpyTag) forms a highly specific and spontaneous isopeptide bond with a 15-kDa protein  
13 (SpyCatcher). The first component of our protein immobilization approach is an engineered  
14 SpyTag-functionalized BIND ECM and the second component is a SpyCatcher protein fused to  
15 another protein of interest. As our arbitrary test protein for ECM-immobilization, we chose GFP.  
16 SpyTag-BIND biofilms were grown on a glass substrate using PHL628 cells and formed  
17 characteristic curli nanofiber networks when either wild-type CsgA or CsgA-SpyTag were  
18 expressed (Fig. 5b-g). We recombinantly produced GFP-SpyCatcher and a non-functional  
19 mutant<sup>28</sup> (GFP-SpyCatcher<sub>E77Q</sub>) and applied cell lysates containing these proteins to SpyTag-  
20 BIND or wild-type CsgA biofilms. Analysis by epifluorescence microscopy revealed, as  
21 expected, that only the combination of biofilms composed of CsgA-SpyTag incubated with GFP-  
22 SpyCatcher resulted in covalent attachment (Fig. 5h). To further validate that the GFP-  
23 SpyCatcher is localized to the extracellular material and not to the cells, we analyzed SpyTag-

BIND + GFP-SpyCatcher samples using confocal microscopy and aligned the high-resolution  
 fluorescence images with SEM micrographs of the same sample (Supplementary Fig, S10a-c).  
 Regions that are fluorescent (Supplementary Fig. S10d,e,g,h) clearly correlate to regions that  
 have a high density of ECM (Supplementary Fig. S10e,f,h,i). These results confirm that the  
 SpyTag peptide can be fused to CsgA and maintain its functionality as a catalytic covalent  
 immobilization tag after extracellular assembly into curli nanofibers. Furthermore, the use of  
 unpurified cell lysate containing the GFP-SpyCatcher fusion protein demonstrates the robust  
 binding specificity between the SpyTag-functionalized curli network and the SpyCatcher fusion  
 protein, even in complex mixtures. This feature of BIND will be especially useful in the  
 development of biocatalysts and biosensors, for the development of a facile and efficient enzyme  
 immobilization process.

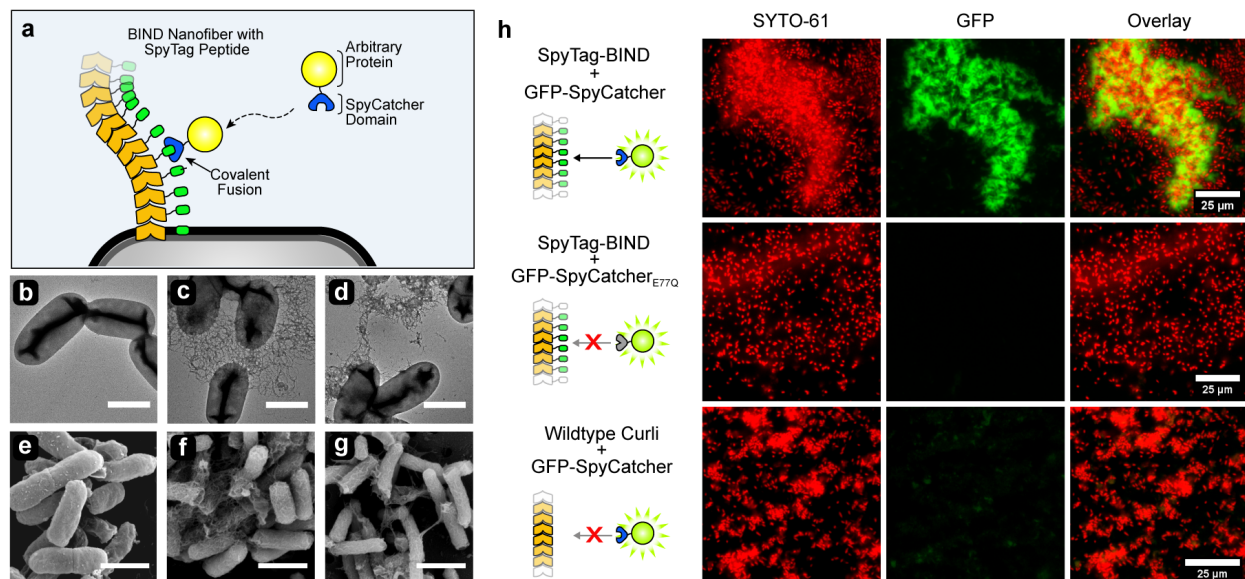


**Figure 5 | Covalent immobilization of full-length proteins onto SpyTag-BIND biofilms.** (a)  
 A schematic showing the protein BIND immobilization strategy which uses an isopeptide bond  
 forming split-protein *S. pyogenes* FbaB adhesin system<sup>28</sup> to covalently attach proteins fused to  
 the SpyCatcher domain onto BIND biofilms displaying the 13-residue SpyTag. TEM and FE-  
 SEM images, respectively, of PHL628-ΔcsgA strains expressing no curli (b, e), wild-type CsgA  
 (c, f), and the SpyTag-BIND biofilms (d, g). All scale bars are 1 μm. (h) SpyTag-BIND biofilms  
 were grown on PLL-modified glass substrates and then visualized with a nucleic-acid stain  
 (SYTO61) followed by incubation with a cell lysate containing GFP-SpyCatcher fusion protein.



Epifluorescence microscopy of the biofilms reveals that only the proper combination of CsgA-SpyTag-BIND biofilms and GFP-SpyCatcher protein-containing cell lysate results in significant protein immobilization (top row). In contrast, SpyTag-BIND biofilms combined with a GFP-SpyCatcher<sub>E77Q</sub> protein that has a key catalytic residue mutated in the SpyCatcher domain showed no immobilization (middle row). Wild-type CsgA biofilms combined with GFP-SpyCatcher also do not show significant immobilization.

**BIND can be used to engineer multifunctional biofilms.** Previous research has shown that cross-seeding between even distantly related amyloid proteins can occur, resulting in composite nanofibers<sup>43</sup>. A key aspect of our BIND system is that by virtue of the random extracellular self-assembly of CsgA monomers, the simultaneous expression of different CsgA fusions will result in a formation of a multifunctional biofilm surface. To demonstrate the generation of a biofilm ECM containing multiple artificially-designed functions, we co-cultured PHL628 cells expressing CsgA-FLAG and CsgA-SpyTag fusion proteins to produce a bifunctional BIND biofilm that can display the FLAG tag as well as immobilize GFP through the SpyTag-SpyCatcher system (Fig. 6). Only the co-cultured sample is able to co-localize the GFP-SpyCatcher and a fluorescently-labeled anti-FLAG antibody, as visualized by confocal microscopy (Fig. 6, bottom row). This capability of engineering multifunctional biofilms greatly increases the utility of our system for complex applications which require any combination of adhesion, display, molecular templating, or protein immobilization.

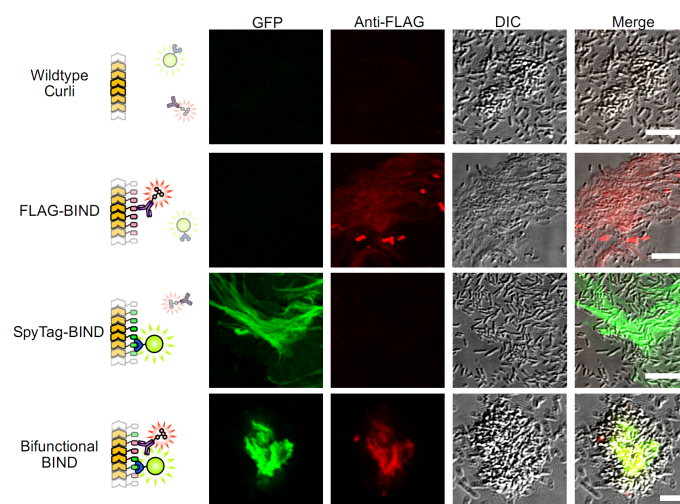


**Figure 6 | BIND can be used to generate programmable multifunctional biofilms.** Wild-type CsgA, FLAG-BIND, SpyTag-BIND, and a co-culture of FLAG-BIND and SpyTag-BIND were all probed with GFP-SpyCatcher followed by anti-FLAG DyLight650 conjugated antibody. Confocal microscopy images for the GFP, DyLight650, and DIC channels are shown. All scale bars are 5 microns.

## Discussion

Here we have demonstrated a strategy, BIND, for the rational molecular design of a microbial extracellular matrix component with the purpose of introducing new function into a biofilm. The biofilms of *E. coli* are partly composed of a functional amyloid nanofiber, curli, which plays a role in bacterial adhesion<sup>37</sup>, aggregation<sup>43</sup>, and biofilm stability<sup>38,44,45</sup>. Our results show that the curli system in *E. coli* is capable of secreting a wide variety of chimeric CsgA-peptide constructs that can self-assemble into the extracellular matrix as amyloid nanofibers. The fused peptide domains are displayed in high density on the network surface and maintain their function even after assembly. The resulting nanofiber networks maintain their ability to encapsulate the cells and show morphological heterogeneity, with some variants exhibiting the tendency to form dense three-dimensional crypt-like structures or expansive fabric-like sheets (Supplementary Fig. S11). Indeed, further exploration of the ability to control the three-dimensional morphology of curli-based nanostructures solely by altering the sequence of CsgA-peptide fusions seems warranted. We then selected three of these artificially designed biofilm materials to demonstrate that three distinct and diverse non-natural functions (silver nanoparticle templating, strong adhesion to steel surfaces, and covalent protein immobilization) can be introduced modularly into *E. coli* biofilms based on the predetermined functions of various engineered peptide sequences. Our results show that biotemplating, substrate adhesion, and protein immobilization can be readily programmed into a bacterial extracellular matrix. Importantly, this was accomplished without the need for system re-optimization, suggesting that other sequences can easily be incorporated into our system to access materials with a vast range of non-natural functions. In addition, a co-culture of cells harboring different CsgA fusions

1 resulted in a bifunctional biofilm, suggesting that the modular aspect of our platform can be used  
2 to engineer biofilms with a wide combination of desired functions.

3         The BIND technology lends itself to the rapid development of interfacial nanomaterials  
4 with functions that can be drawn from the diverse repertoire of known natural and artificial  
5 peptides and proteins. These biofilm-based materials can be used in a wide range of  
6 environments that may or may not be conducive to cellular survival. In hospitable environments,  
7 the encapsulated cells of the biofilm may be induced to self-regenerate or heal the material over  
8 time, or remodel the material in response to environmental cues. In harsher environments, the  
9 highly robust amyloid matrix, once assembled, could persist beyond the lifetime of the cellular  
10 components as an acellular structure without the need for maintenance. In principle, our  
11 approach can be used to introduce new function to many other microbial biofilms with analogous  
12 functional amyloids (e.g., *Salmonella*<sup>46</sup>, *Pseudomonas*<sup>47</sup>, *Bacillus*<sup>48</sup> spp.) to capitalize on the  
13 particular features of each wild-type strain. Given that the engineered bacteria proliferate rapidly  
14 and require no petroleum-derived raw building blocks in order to biosynthesize the external  
15 matrix, BIND may be useful as a scalable and green approach to fabricating customized  
16 interfacial materials across a wide range of size scales and environments.

17         Recent work with synthetic gene circuits allows for the control of biofilm formation  
18 and dispersal dynamics through the engineering of global biofilm regulatory proteins<sup>7,49,50</sup>. Other  
19 work has paved the way for the patterning and control of curli composition<sup>14</sup>. By combining such  
20 biofilm control strategies with the ability to widely program the functional properties of the  
21 extracellular matrix as we present here with BIND platform, we envision a merging of synthetic  
22 biology and materials science approaches. This would allow the development of large-scale  
23 programmable ‘living’ materials in which bacteria act as autonomous and self-replicating



distributed molecular factories for the production of large-scale materials. Additionally, engineered complex genetic logic gates could be used to switch on one or more defined BIND biofilms under specific environmental cues. This would potentially allow a single cell to encode for tens and possibly hundreds of different artificial BIND variants that could dynamically alter the bacterial ECM properties on demand.

## Methods

**Cell strains and plasmids.** All cloning and protein expression was performed in Mach1 (Life Technologies, CA, USA) and Rosetta cells (EMD Millipore, CA, USA), respectively. The *csgA* gene was isolated from *E. coli* K-12 genomic DNA and cloned into pBbE1a<sup>51</sup>, a ColE1 plasmid under control of the Trc promoter. Peptide insert regions were either fully synthesized (Integrated DNA Technologies, IA, USA) or PCR-generated by overlap extension<sup>52</sup>. All cloning was performed using isothermal Gibson Assembly<sup>53</sup> and verified by DNA sequencing. The *csgA* deletion mutant LSR10 (MC4100,  $\Delta csgA$ ) was a kind gift from the Chapman Laboratory. The *csgA* deletion mutant PHL628- $\Delta csgA$  (MG1655, *malA-Kan ompR234*  $\Delta csgA$ ) was provided by the Hay Laboratory. All cell strains, plasmids, and primers used in this study are fully provided in the supplementary section (Supplementary Tables S1, S2, and S3).

**Curli biofilm formation.** To produce curli, LSR10 cells or PHL628 cells were transformed with pBbE1a plasmids encoding for CsgA or CsgA-peptide fusions. As a negative control, cells were transformed with empty pBbE1a plasmid. The cells were then streaked or spotted onto YESCA-CR plates<sup>54</sup>, containing 10 g/L of casamino acids, 1 g/L of yeast extract, and 20 g/L of agar. These plates were supplemented with 100  $\mu$ g/mL of ampicillin, 0.5 mM of IPTG, 25  $\mu$ g/mL of Congo Red and 5  $\mu$ g/mL of Brilliant Blue G250. The plates were then incubated for 48 hours at

25°C and then imaged to determine the extent of Congo Red binding. For the spotted plates, the transformants were grown in YESCA liquid media supplemented with 100 µg/mL of ampicillin and 0.2 mM of IPTG for 48 hours at 25°C before spotting 20 µL onto YESCA-CR plates.

**Scanning electron microscopy.** Curliated wild-type or BIND cell samples were either directly taken from induced YESCA cultures or scraped from YESCA-CR plates and resuspended in millipore H<sub>2</sub>O. For SEM analysis, samples were applied to Nuclepore filters under vacuum, washed with millipore H<sub>2</sub>O and fixed with 2% glutaraldehyde + 2% paraformaldehyde overnight at 4°C, followed by fixation in 1% osmium tetroxide. The samples were then washed in millipore H<sub>2</sub>O, dehydrated with an increasing ethanol step gradient, followed by a hexamethyldisilazane step gradient before gold sputtering and analysis on a Zeiss Supra55VP FE-SEM.

**Transmission electron microscopy.** Curliated wild-type or BIND cell samples were either directly taken from induced YESCA liquid cultures or scraped from YESCA-CR plates and resuspended into millipore H<sub>2</sub>O. For TEM analysis, 5 µL of the sample was spotted onto formvar-carbon grids (Electron Microscopy Sciences, PA, USA), washed with millipore H<sub>2</sub>O, and stained with 1% uranyl formate before analysis on a JEOL 1200 TEM.

**Whole-cell filtration ELISA.** To quantitatively detect the presence of extracellular CsgA as high-molecular weight assemblies, an adapted whole-cell filtration ELISA protocol for detecting bacterial surface antigens was used<sup>55</sup>. BIND transformants were used to inoculate 3 mL YESCA liquid cultures supplemented with 50 µg/mL of carbenicillin, grown to mid-log phase, and induced with 0.25 mM of IPTG. The induced cells were incubated at 25°C for 48 hours before analysis. The cultures were subsequently placed on ice and all were diluted to an OD<sub>600</sub> of 0.1 using Tris-buffered saline (TBS). Sodium azide was added to 0.1% to inhibit cell metabolism. All To a Multiscreen-GV 96-well filter plate (0.22 µm pore size; EMD Millipore, CA, USA), 25

1     $\mu\text{L}$  of the diluted culture was added and washed three times in Wash Buffer (TBS + 0.1%  
2    Tween-20 + 0.1%  $\text{NaN}_3$ ) and incubated in 200  $\mu\text{L}$  of Blocking Buffer (wash buffer  
3    supplemented with 1% bovine serum albumin and 0.01%  $\text{H}_2\text{O}_2$ ) for 1 hour at 37°C. The  $\text{H}_2\text{O}_2$  is  
4    needed to inactivate endogenous cellular peroxidases<sup>55</sup>. The samples were then washed three  
5    times in Wash Buffer, incubated with anti-CsgA primary antibody<sup>8</sup> diluted to 1:10,000 in Wash  
6    Buffer for 1 hour at 25°C, washed three more times in Wash Buffer, and then incubated with  
7    goat anti-rabbit HRP-conjugated secondary antibody (Thermo Fisher Scientific, MA, USA)  
8    diluted to 1:5,000 in Wash Buffer for 1 hour at 25°C. After a final washing step three times in  
9    Wash Buffer, the samples were processed using the Ultra-TMB (3,3',5,5'-  
10    tetramethylbenzidine) ELISA substrate (Thermo Fisher Scientific, MA, USA), adding 100  $\mu\text{L}$   
11    per well. After incubation at room temperature for 5 minutes, the reaction was terminated by the  
12    addition of 50  $\mu\text{L}$  of 2M  $\text{H}_2\text{SO}_4$ . Exactly 100  $\mu\text{L}$  of this reaction was transferred to a flat-well  
13    bottom 96-well plate and analyzed on a BioTek Synergy H1 Multi-Mode Plate Reader,  
14    measuring the absorbance at 450 nm and a reference wavelength of 650 nm.

15    **MBD-BIND binding to 304L stainless steel coupons.** Steel alloy 304L coupons (Alabama  
16    Specialty Products, Inc., AL, USA) were cleaned with fine-grit sandpaper, acetone, millipore  
17    water, sonicated in 1M NaOH for 1 hour at 80°C, washed again with millipore water, and finally  
18    rinsed with acetone before air-drying. PHL628  $\Delta\text{csgA}$  transformants were grown in YESCA  
19    media as described above and induced by adding 0.5 mM IPTG and 3% DMSO for 48 hours at  
20    25°C, 150 rpm. Cell cultures were normalized to an  $\text{OD}_{600}$  of 1 and 20  $\mu\text{L}$  was spotted onto a  
21    304L coupon. The spotted coupon was placed in a sterile petri dish and placed in 4°C to allow  
22    attachment and minimize evaporation. After 48 hours, the coupons were rinsed briefly with

PBST, placed in a tube filled with PBST, and vigorously vortexed thrice for 30 seconds. The coupons were then fixed and SEM imaged according to the protocols described above.

**Silver nanoparticle templating.** PHL628-*ΔcsgA* cells were transformed with wild-type CsgA, and CsgA-A3 expressing plasmids and induced with 0.2 mM IPTG in YESCA broth containing 100 µg/mL carbenicillin for 48 hours. The cells and curli were isolated by pelleting and then resuspended in PBS+CM. Nickle-formvar/carbon TEM grids were floated on drops of these resuspended samples, washed twice with PBS+CM, three times with millipore H<sub>2</sub>O, and then incubated on a drop containing 147 mM AgNO<sub>3</sub> for 4 hours. The grids were then washed thrice with mpH<sub>2</sub>O and negatively stained and analyzed by TEM as described above. Incubation with lower amounts of AgNO<sub>3</sub> for longer periods of time resulted in substantial cell lysis, complicating analysis.

**Biofilm fluorescence microscopy imaging.** PHL628-*ΔcsgA* cells transformed with control, wild-type CsgA, and CsgA-SpyTag expressing plasmids were grown up in 20 mL YESCA broth containing 100 µg/mL ampicillin at 30°C until an OD of 0.6. Plasma-activated and PLL-functionalized coverslips were placed into the cultures and curli expression and biofilm formation were induced by adding 0.5 mM IPTG and 3% DMSO. Cultures were grown at 25°C and 150 rpm for 48 hours. Slides were removed from the cultures and washed 3x 20 min in wash buffer (1x PBS+0.5% Tween 20), shaking at 150 rpm. After the washes, 0.5 mL of 1 mg/mL GFP-SpyCatcher- or GFP-SpyCatcher(E77Q)-containing cell lysate solution (in PBS+1% BSA+0.5% Tween) was added to slides. The biofilms were incubated for 1 hour and then washed 2x 20 min with wash buffer. The samples were then stained with SYTO-61 (10 µM) for 20 min and washed with wash buffer 2x15 min shaking at 150 rpm. Slides were then imaged in epifluorescence mode on a Leica TIRF DM16000B at 60x and 100x. For the multifunctional

1 BIND experiments, cells at an initial OD600 of 2.5 were cultured in MatTek glass-bottom dishes  
2 for 72 hours under inducing conditions (YESCA / 0.5 mM IPTG / 100 ng/mL carbenicillin / 3%  
3 DMSO). The biofilms were then washed 3x 10 min in PBST, blocked with 1% BSA in PBST for  
4 1 hour, and incubated with GFP-SpyCatcher-containing clarified cell lysate for 1 hour. The  
5 dishes were then extensively washed with 0.1% BSA + PBST under gentle shaking before  
6 incubation with an anti-FLAG DyLight 680 antibody (Pierce) for 1 hour. The samples were  
7 washed as before with 0.1% BSA + PBST, fixed with 2% glutaraldehyde + 2%  
8 paraformaldehyde in 0.1M sodium cacodylate buffer for 15 minutes, and then incubated in  
9 PBS+10 mM glycine overnight at 4°C to eliminate autofluorescence. All multifunctional BIND  
10 samples were analyzed on Leica SP5 X MP Inverted Confocal Microscope with identical laser  
11 power and detector integration settings.

## References

1. Flemming, H.C. & Wingender, J. The biofilm matrix. *Nat Rev Microbiol* **8**, 623-33 (2010).
2. Römling, U. & Balsalobre, C. Biofilm infections, their resilience to therapy and innovative treatment strategies. *J Intern Med* **272**, 541-61 (2012).
3. Logan, B.E. Exoelectrogenic bacteria that power microbial fuel cells. *Nat Rev Microbiol* **7**, 375-81 (2009).
4. Singh, R., Paul, D. & Jain, R.K. Biofilms: implications in bioremediation. *Trends Microbiol* **14**, 389-97 (2006).
5. Halan, B., Buehler, K. & Schmid, A. Biofilms as living catalysts in continuous chemical syntheses. *Trends Biotechnol* **30**, 453-65 (2012).
6. Tsoligkas, A.N. *et al.* Engineering biofilms for biocatalysis. *Chembiochem* **12**, 1391-5 (2011).
7. Hong, S.H. *et al.* Synthetic quorum-sensing circuit to control consortial biofilm formation and dispersal in a microfluidic device. *Nat Commun* **3**, 613 (2012).
8. Chapman, M.R. *et al.* Role of *Escherichia coli* curli operons in directing amyloid fiber formation. *Science* **295**, 851-5 (2002).
9. Hammar, M., Arnqvist, A., Bian, Z., Olsén, A. & Normark, S. Expression of two *csg* operons is required for production of fibronectin- and congo red-binding curli polymers in *Escherichia coli* K-12. *Mol Microbiol* **18**, 661-70 (1995).
10. Smith, J.F., Knowles, T.P., Dobson, C.M., Macphée, C.E. & Welland, M.E. Characterization of the nanoscale properties of individual amyloid fibrils. *Proc Natl Acad Sci U S A* **103**, 15806-11 (2006).
11. Larsen, P., Nielsen, J.L., Otzen, D. & Nielsen, P.H. Amyloid-like adhesins produced by floc-forming and filamentous bacteria in activated sludge. *Appl Environ Microbiol* **74**, 1517-26 (2008).
12. Sivanathan, V. & Hochschild, A. Generating extracellular amyloid aggregates using *E. coli* cells. *Genes Dev* **26**, 2659-67 (2012).
13. Van Gerven, N. *et al.* Secretion and functional display of fusion proteins through the curli biogenesis pathway. *Mol Microbiol* (2014).
14. Chen, A.Y. *et al.* Synthesis and patterning of tunable multiscale materials with engineered cells. *Nat Mater* **13**, 515-23 (2014).
15. Giltner, C.L. *et al.* The *Pseudomonas aeruginosa* type IV pilin receptor binding domain functions as an adhesin for both biotic and abiotic surfaces. *Mol Microbiol* **59**, 1083-96 (2006).
16. Marcus, A., Sadimin, E., Richardson, M., Goodell, L. & Fyfe, B. Fluorescence microscopy is superior to polarized microscopy for detecting amyloid deposits in Congo red-stained trephine bone marrow biopsy specimens. *Am J Clin Pathol* **138**, 590-3 (2012).
17. Casadaban, M.J. Transposition and fusion of the *lac* genes to selected promoters in *Escherichia coli* using bacteriophage lambda and Mu. *J Mol Biol* **104**, 541-55 (1976).
18. Zogaj, X., Nimtz, M., Rohde, M., Bokranz, W. & Römling, U. The multicellular morphotypes of *Salmonella typhimurium* and *Escherichia coli* produce cellulose as the second component of the extracellular matrix. *Mol Microbiol* **39**, 1452-63 (2001).
19. Liu, D. & Reeves, P.R. *Escherichia coli* K12 regains its O antigen. *Microbiology* **140** ( Pt 1), 49-57 (1994).

- 1 20. Teather, R.M. & Wood, P.J. Use of Congo red-polysaccharide interactions in enumeration  
2 and characterization of cellulolytic bacteria from the bovine rumen. *Appl Environ Microbiol*  
3 **43**, 777-80 (1982).
- 4 21. Hochuli, E., Bannwarth, W., Dobeli, H., Gentz, R. & Stuber, D. Genetic approach to  
5 facilitate purification of recombinant proteins with a novel metal chelate adsorbent. *Nat*  
6 *Biotech* **6**, 1321-1325 (1988).
- 7 22. Kim, S.N. *et al.* Preferential binding of peptides to graphene edges and planes. *J Am Chem*  
8 *Soc* **133**, 14480-3 (2011).
- 9 23. Hopp, T.P. *et al.* A Short Polypeptide Marker Sequence Useful for Recombinant Protein  
10 Identification and Purification. *Nat Biotech* **6**, 1204-1210 (1988).
- 11 24. Pender, M.J., Sowards, L.A., Hartgerink, J.D., Stone, M.O. & Naik, R.R. Peptide-mediated  
12 formation of single-wall carbon nanotube composites. *Nano Lett* **6**, 40-4 (2006).
- 13 25. Naik, R.R., Stringer, S.J., Agarwal, G., Jones, S.E. & Stone, M.O. Biomimetic synthesis  
14 and patterning of silver nanoparticles. *Nat Mater* **1**, 169-72 (2002).
- 15 26. Chung, W.J., Kwon, K.Y., Song, J. & Lee, S.W. Evolutionary screening of collagen-like  
16 peptides that nucleate hydroxyapatite crystals. *Langmuir* **27**, 7620-8 (2011).
- 17 27. Oren, E.E. *et al.* A novel knowledge-based approach to design inorganic-binding peptides.  
18 *Bioinformatics* **23**, 2816-22 (2007).
- 19 28. Zakeri, B. *et al.* Peptide tag forming a rapid covalent bond to a protein, through engineering  
20 a bacterial adhesin. *Proc Natl Acad Sci U S A* **109**, E690-7 (2012).
- 21 29. Zhou, W., Schwartz, D.T. & Baneyx, F. Single-pot biofabrication of zinc sulfide immuno-  
22 quantum dots. *J Am Chem Soc* **132**, 4731-8 (2010).
- 23 30. Houston, M.E. *et al.* Binding of an oligopeptide to a specific plane of ice. *J Biol Chem* **273**,  
24 11714-8 (1998).
- 25 31. Arakaki, A., Webb, J. & Matsunaga, T. A novel protein tightly bound to bacterial magnetic  
26 particles in Magnetospirillum magneticum strain AMB-1. *J Biol Chem* **278**, 8745-50  
27 (2003).
- 28 32. Taylor, J.D. *et al.* Atomic Resolution Insights into Curli Fiber Biogenesis. *Structure* **19**,  
29 1307-1316 (2011).
- 30 33. Sabaté, R. & Ventura, S. Cross- $\beta$ -sheet supersecondary structure in amyloid folds:  
31 techniques for detection and characterization. *Methods Mol Biol* **932**, 237-57 (2013).
- 32 34. Schütz, A.K. *et al.* The amyloid-Congo red interface at atomic resolution. *Angew Chem Int*  
33 *Ed Engl* **50**, 5956-60 (2011).
- 34 35. Sivanathan, V. & Hochschild, A. A bacterial export system for generating extracellular  
35 amyloid aggregates. *Nat Protoc* **8**, 1381-90 (2013).
- 36 36. Gebbink, M.F., Claessen, D., Bouma, B., Dijkhuizen, L. & Wösten, H.A. Amyloids--a  
37 functional coat for microorganisms. *Nat Rev Microbiol* **3**, 333-41 (2005).
- 38 37. Hidalgo, G., Chen, X., Hay, A.G. & Lion, L.W. Curli produced by Escherichia coli  
39 PHL628 provide protection from Hg(II). *Appl Environ Microbiol* **76**, 6939-41 (2010).
- 40 38. Vidal, O. *et al.* Isolation of an Escherichia coli K-12 mutant strain able to form biofilms on  
41 inert surfaces: involvement of a new ompR allele that increases curli expression. *J Bacteriol*  
42 **180**, 2442-9 (1998).
- 43 39. Reguera, G. *et al.* Extracellular electron transfer via microbial nanowires. *Nature* **435**,  
44 1098-101 (2005).
- 45 40. Hochbaum, A.I. & Aizenberg, J. Bacteria pattern spontaneously on periodic nanostructure  
46 arrays. *Nano Lett* **10**, 3717-21 (2010).

41. Lewandowski, Z., Beyenal, H., Myers, J. & Stookey, D. The effect of detachment on biofilm structure and activity: the oscillating pattern of biofilm accumulation. *Water Sci Technol* **55**, 429-36 (2007).
42. Horn, H., Reiff, H. & Morgenroth, E. Simulation of growth and detachment in biofilm systems under defined hydrodynamic conditions. *Biotechnol Bioeng* **81**, 607-17 (2003).
43. Zhou, Y. *et al.* Promiscuous cross-seeding between bacterial amyloids promotes interspecies biofilms. *J Biol Chem* (2012).
44. Pawar, D.M., Rossmann, M.L. & Chen, J. Role of curli fimbriae in mediating the cells of enterohaemorrhagic *Escherichia coli* to attach to abiotic surfaces. *J Appl Microbiol* **99**, 418-25 (2005).
45. Kikuchi, T., Mizunoe, Y., Takade, A., Naito, S. & Yoshida, S. Curli fibers are required for development of biofilm architecture in *Escherichia coli* K-12 and enhance bacterial adherence to human uroepithelial cells. *Microbiol Immunol* **49**, 875-84 (2005).
46. White, A.P. *et al.* High efficiency gene replacement in *Salmonella enteritidis*: chimeric fimbrins containing a T-cell epitope from *Leishmania major*. *Vaccine* **17**, 2150-61 (1999).
47. Dueholm, M.S. *et al.* Functional amyloid in *Pseudomonas*. *Mol Microbiol* (2010).
48. Romero, D., Aguilar, C., Losick, R. & Kolter, R. Amyloid fibers provide structural integrity to *Bacillus subtilis* biofilms. *Proc Natl Acad Sci U S A* **107**, 2230-4 (2010).
49. Ma, Q., Yang, Z., Pu, M., Peti, W. & Wood, T.K. Engineering a novel c-di-GMP-binding protein for biofilm dispersal. *Environ Microbiol* **13**, 631-42 (2011).
50. Hong, S.H., Lee, J. & Wood, T.K. Engineering global regulator Hha of *Escherichia coli* to control biofilm dispersal. *Microb Biotechnol* **3**, 717-28 (2010).
51. Lee, T.S. *et al.* BglBrick vectors and datasheets: A synthetic biology platform for gene expression. *J Biol Eng* **5**, 12 (2011).
52. Horton, R.M., Hunt, H.D., Ho, S.N., Pullen, J.K. & Pease, L.R. Engineering hybrid genes without the use of restriction enzymes: gene splicing by overlap extension. *Gene* **77**, 61-8 (1989).
53. Gibson, D.G. *et al.* Enzymatic assembly of DNA molecules up to several hundred kilobases. *Nat Methods* **6**, 343-5 (2009).
54. Benhold, H. Specific staining of amyloid by Congo red. *Muenchen. Med. Wochenschr.*, 1537-1538 (1922).
55. Itoh, S. *et al.* New rapid enzyme-linked immunosorbent assay to detect antibodies against bacterial surface antigens using filtration plates. *Biol Pharm Bull* **25**, 986-90 (2002).

## Acknowledgements

This work was funded by the Wyss Institute for Biologically Inspired Engineering. Z.B. acknowledges the NSF GRF for funding. P.R.T. is grateful for funding from the A\*STAR National Science Graduate Fellowship (Singapore). The authors thank Professor Matthew R. Chapman (University of Michigan) for the kind donation of the LSR10 *E. coli* strain, the anti-CsgA antibody, and assistance with technical queries. The authors also thank Professor Anthony



1 G. Hay (Cornell University) for providing the PHL628-*ΔcsgA* strain. The AgfA homology model  
2 protein structure was graciously provided by Professor Aaron P. White (University of  
3 Saskatchewan).

#### 4 **Author Contributions**

5 P.Q.N and N.S.J. conceived of the concept, designed the research, and analyzed the data.

6 P.Q.N., Z.B., and P.R.T. performed research and analyzed the data. P.Q.N. and N.S.J. wrote the  
7 paper with discussions and contributions from all other authors. All authors discussed the results  
8 and commented on the manuscript.

#### 9 **Competing Financial Interests**

10 The authors have applied for a patent based on this work